# The Impact of Noise Correlation and Channel Phase Information on the Data-Rate

# of the Single-Symbol ML Decodable Distributed STBCs

Zhihang Yi and Il-Min Kim, *Senior Member, IEEE*

Department of Electrical and Computer Engineering

Queen's University

Kingston, Ontario, K7L 3N6

Canada

Email: ilmin.kim@queensu.ca

**Abstract**

Very recently, we proposed the row-monomial distributed orthogonal space-time block codes (DOSTBCs) and showed that the row-monomial DOSTBCs achieved approximately twice higher bandwidth efficiency than the repetition-based cooperative strategy [1]. However, we imposed two limitations on the row-monomial DOSTBCs. The first one was that the associated matrices of the codes must be row-monomial. The other was the assumption that the relays did not have any channel state information (CSI) of the channels from the source to the relays, although this CSI could be readily obtained at the relays without any additional pilot signals or any feedback overhead. In this paper, we first remove the row-monomial limitation; but keep the CSI limitation. In this case, we derive an upper bound of the data-rate of the DOSTBC and it is larger than that of the row-monomial DOSTBCs in [1]. Secondly, we abandon the CSI limitation; but keep the row-monomial limitation. Specifically, we propose the row-monomial DOSTBCs with channel phase information (DOSTBCs-CPI) and derive an upper bound of the data-rate of those codes. The row-monomial DOSTBCs-CPI have higher data-rate than the DOSTBCs and the row-monomial DOSTBCs. Furthermore, we find the actual row-monomial DOSTBCs-CPI which achieve the upper bound of the data-rate.

*Index Terms*—Cooperative networks, distributed space-time block codes, diversity, single-symbol maximum likelihood decoding.

## I. INTRODUCTION

In a cooperative network, the relays cooperate to help the source transmit the information-bearing symbols to the destination. The relay cooperation improves the performance of the network considerably [2]–[5]. The cooperative strategy of the relays is crucial and it decides the performance of a cooperative network. A simple cooperative strategy is the *repetition-based cooperative strategy* which was proposed in [4] and studied in [7]–[11]. This cooperative strategy achieves the full diversity order in the number $K$ of relays.[1] Furthermore, the maximum likelihood (ML) decoding at the destination is single-symbol ML decodable.[2] However, the repetition-based cooperative strategy has poor bandwidth efficiency, since its data-rate[3] is just $1/K$. Many works have been devoted to improve the bandwidth efficiency of the cooperative networks, such as the cooperative beamforming [12], [13], and the relay selection [14]–[16]. More attentions have been given to the *distributed space-time codes* (DSTCs) [17]–[19]. Furthermore, many practical DSTCs have been proposed in [20]–[26]. Although all those codes could improve the bandwidth efficiency, they were not single-symbol ML decodable in general, and hence, they had much higher decoding complexities than the repetition-based cooperative strategy.

Very few works have tried to propose the DSTCs achieving the single-symbol ML decodability and the full diversity order. In [27], Hua *et al.* used the existing orthogonal designs in cooperative networks; but they found that most codes were not single-symbol ML decodable any more. In [28], Rajan *et al.* used the clifford unitary weight single-symbol decodable codes in cooperative networks. The codes were single-symbol ML decodable only when there were four relays. Moreover, the codes could not achieve the full diversity order in an arbitrary signal constellation. In [29], Jing *et al.* applied the orthogonal and quasi-orthogonal designs in cooperative networks and they analyzed the diversity order of the codes. The authors of [29] claimed that the codes achieved the single-symbol ML decodability as long as the noises at the destination were uncorrelated. However, we noticed that the rate-$3/4$ code given in [29] was actually not single-symbol ML decodable, although it generated uncorrelated noises at the destination. Actually in this paper, we will show that, when the noises are uncorrelated, the codes have to satisfy another constraint in order to be single-symbol ML decodable.

Only very recently, the DSTCs achieving the single-symbol ML decodability have been studied. In [1], we proposed the distributed orthogonal space-time block codes (DOSTBCs), and we showed that the DOSTBCs achieved the single-symbol ML decodability and the full diversity order. Moreover, we systematically studied some special DOSTBCs, namely the row-monomial DOSTBCs, which generated uncorrelated noises at the destination. Specifically, an upper bound of the data-rate of the row-monomial DOSTBC was derived. This upper bound suggested that the row-monomial DOSTBCs had approximately twice higher bandwidth efficiency than the

---

[1]In this paper, unless otherwise indicated, saying one code or one scheme achieves the full diversity order means it achieves the full diversity in an arbitrary signal constellation.

[2]A code or a scheme is single-symbol ML decodable, if its ML decoding metric can be written as a sum of multiple terms, each of which depends on at most one transmitted information-bearing symbol [6].

[3]In this paper, the data-rate of a cooperative strategy or a distributed space-time code is equal to the ratio of the number of transmitted information-bearing symbols to the number of time slots used by the relays to transmit all these symbols.

repetition-based cooperative strategy. In [1], however, we imposed two limitations on the row-monomial DOSTBCs, in order to simplify the analysis. The first one was that the associated matrices of the codes must be row-monomial[4], which ensured uncorrelated noises at the destination. The other was the assumption that the relays did not have any channel state information (CSI) of the channels from the source to the relays, i.e. the channels of the first hop. Actually, since we assumed the destination had the CSI of the channels from the source to the relays and the channels from the relays to the destination in [1], the CSI of the first hop could be easily obtained at the relays without requiring additional pilot signals or any feedback overhead. But, it is still unknown what impact those two limitations have on the data-rate of the codes. This has motivated our work.

In this paper, we first abandon the row-monomial limitation; but keep the CSI limitation. That is, we consider the DOSTBCs where the noises at the destination are possibly correlated and the relays do not have any CSI of the first hop. We derive an upper bound of the data-rate of the DOSTBC and it is larger than that of the row-monomial DOSTBC in [1]. This implies that the DOSTBCs can potentially improve the bandwidth efficiency of the cooperative network. But, like the row-monomial DOSTBCs, the DOSTBCs may not have good bandwidth efficiency in a cooperative network with many relays, because the upper bound of the data-rate of the DOSTBC decreases with the number $K$ of relays. Secondly, we remove the CSI limitation; but keep the row-monomial limitation. Specifically, the relays know the channel phase information (CPI) of the first hop and use this information in the code construction. Those codes are referred to as the *row-monomial DOSTBCs with CPI* (DOSTBCs-CPI). We derive an upper bound of the data-rate of the row-monomial DOSTBC-CPI and also find the actual codes achieving this upper bound. The upper bound of the data-rate of the row-monomial DOSTBC-CPI is higher than those of the DOSTBCs and the row-monomial DOSTBCs. Thus, the row-monomial DOSTBCs-CPI have better bandwidth efficiency than the DOSTBCs and the row-monomial DOSTBCs. Furthermore, the upper bound of the data-rate of the row-monomial DOSTBC-CPI is independent of the number $K$ of relays, which ensures the codes have good bandwidth efficiency even when there are many relays.

The rest of this paper is organized as follows. Section II describes the cooperative network considered in this paper. In Section III, we remove the row-monomial limitation; but the relays do have any CSI. Specifically, we study the DOSTBCs and derive an upper bound of the data-rate of the DOSTBC. In Section IV, the relays exploit the CPI to construct the codes; but the row-monomial limitation is maintained. Specifically, we first define the row-monomial DOSTBCs-CPI and then derive an upper bound of the data-rate of the row-monomial DOSTBC-CPI. We present some numerical results in Section V and conclude this paper in Section VI.

*Notations:* Bold upper and lower letters denote matrices and row vectors, respectively. Also, $\mathrm{diag}[x_1, \cdots, x_K]$ denotes the $K \times K$ diagonal matrix with $x_1, \cdots, x_K$ on its main diagonal; $\mathbf{0}$ the all-zero matrix; $\boldsymbol{I}$ the identity matrix; $\det(\cdot)$ the determinant of a matrix; $[\cdot]_k$ the $k$-th entry of a vector; $[\cdot]_{k_1,k_2}$ the $(k_1, k_2)$-th entry of a matrix; $(\cdot)^*$ the complex conjugate; $(\cdot)^H$ the Hermitian; $(\cdot)^T$ the transpose. Let $\boldsymbol{X} = [\boldsymbol{x}_1; \cdots; \boldsymbol{x}_K]$ denote the matrix with $\boldsymbol{x}_k$ as its $k$-th row, $1 \leq k \leq K$. For a real number $a$, $\lceil a \rceil$ denotes the ceiling function of $a$.

---

[4]A matrix is said to be row-monomial (column-monomial) if there is at most one non-zero entry on every row (column) of it [30].

## II. SYSTEM MODEL

Consider a cooperative network with one source, $K$ relays, and one destination. Every terminal has only one antenna and is half-duplex. Denote the channel from the source to the $k$-th relay by $h_k$ and the channel from the $k$-th relay to the destination by $f_k$, where $h_k$ and $f_k$ are spatially uncorrelated complex Gaussian random variables with zero mean and unit variance. We assume that the destination has full CSI, i.e. it knows the instantaneous values of $h_k$ and $f_k$ by using pilot signals; while the source has no CSI. The relays may have partial CSI and this will be discussed in detail later.

At the beginning, the source transmits $N$ complex-valued information-bearing symbols over $N$ consecutive time slots.[5] Let $\boldsymbol{s} = [s_1, \cdots, s_N]$ denote the information-bearing symbol vector transmitted from the source, where the power of $s_n$ is $E_s$. Assume the coherence time of $h_k$ is larger than $N$; then the received signal vector $\boldsymbol{y}_k$ at the $k$-th relay is $\boldsymbol{y}_k = h_k \boldsymbol{s} + \boldsymbol{n}_k$, where $\boldsymbol{n}_k = [n_{k,1}, \cdots, n_{k,N}]$ is the additive noise at the $k$-th relay and it is uncorrelated complex Gaussian with zero mean and identity covariance matrix. All the relays are working in the amplify-and-forward mode and the amplifying coefficient $\rho$ is $\sqrt{E_r/(1+E_s)}$ for every relay, where $E_r$ is the transmission power at every relay.[6] Based on the received signal vector $\boldsymbol{y}_k$, the $k$-th relay produces a transmitted signal vector and forwards it to the destination.

Firstly, we present the system model of the DOSTBCs, which will be studied in Section III. We assume that the $k$-th relay has no CSI of the first hop. This can be true when the relays do not have any channel estimation devices due to strict power and/or size constraints.[7] Then the $k$-th relay produces the transmitted signal vector $\boldsymbol{x}_k^D$ as follows:

$$\begin{aligned} \boldsymbol{x}_k^D &= \rho(\boldsymbol{y}_k \boldsymbol{A}_k + \boldsymbol{y}_k^* \boldsymbol{B}_k) \\ &= \rho h_k \boldsymbol{s} \boldsymbol{A}_k + \rho h_k^* \boldsymbol{s}^* \boldsymbol{B}_k + \rho \boldsymbol{n}_k \boldsymbol{A}_k + \rho \boldsymbol{n}_k^* \boldsymbol{B}_k. \end{aligned} \tag{1}$$

The matrices $\boldsymbol{A}_k$ and $\boldsymbol{B}_k$ are called the associated matrices. They have the dimension of $N \times T$ and their properties will be discussed in detail later. Assume the coherence time of $f_k$ is larger than $T$. The received signal vector at

[5]If the information-bearing symbols are real-valued, one can use the rate-one generalized real orthogonal design proposed by [31] in the cooperative networks without any changes. The codes achieve the single-symbol ML decodability and the full diversity order [27]. Therefore, we focus on the complex-valued symbols in this paper.

[6]We set $\rho = \sqrt{E_r/(1+E_s)}$ as in many previous publications including [18], [23], [28], [29]. This ensures the average transmission power of every relay is $E_r$ in a long term.

[7]Even when the relays can not estimate the channels, the destination is still able to obtain the full CSI. This is because the destination usually dose not have any power or size limitation, and hence, it can be equipped with sophisticated channel estimation devices. Furthermore, although the relays can not estimate the channels, they can forward the pilot signals from the source to the destination, and they can transmit their own pilot signals to the destination. Based on those pilot signals, the destination is able to obtain the full CSI, which has been discussed in [16] and [27].

the destination is given by

$$
\begin{aligned}
\boldsymbol{y}_D &= \sum_{k=1}^{K} f_k \boldsymbol{x}_k^D + \boldsymbol{n}_d \\
&= \sum_{k=1}^{K} (\rho f_k h_k \boldsymbol{s} \boldsymbol{A}_k + \rho f_k h_k^* \boldsymbol{s}^* \boldsymbol{B}_k) + \sum_{k=1}^{K} (\rho f_k \boldsymbol{n}_k \boldsymbol{A}_k + \rho f_k \boldsymbol{n}_k^* \boldsymbol{B}_k) + \boldsymbol{n}_d,
\end{aligned} \tag{2}
$$

where $\boldsymbol{n}_d = [n_{d,1}, \cdots, n_{d,T}]$ is the additive noise at the destination and it is uncorrelated complex Gaussian with zero mean and identity covariance matrix.[8] Define $\boldsymbol{w}_D$, $\boldsymbol{X}_D$, and $\boldsymbol{n}_D$ as follows:

$$
\boldsymbol{w}_D = [\rho f_1, \cdots, \rho f_K] \tag{3}
$$

$$
\boldsymbol{X}_D = [h_1 \boldsymbol{s} \boldsymbol{A}_1 + h_1^* \boldsymbol{s}^* \boldsymbol{B}_1; \cdots; h_K \boldsymbol{s} \boldsymbol{A}_K + h_K^* \boldsymbol{s}^* \boldsymbol{B}_K] \tag{4}
$$

$$
\boldsymbol{n}_D = \sum_{k=1}^{K} (\rho f_k \boldsymbol{n}_k \boldsymbol{A}_k + \rho f_k \boldsymbol{n}_k^* \boldsymbol{B}_k) + \boldsymbol{n}_d; \tag{5}
$$

then we can rewrite (2) in the following way

$$
\boldsymbol{y}_D = \boldsymbol{w}_D \boldsymbol{X}_D + \boldsymbol{n}_D. \tag{6}
$$

Furthermore, from (5), it is easy to see that the mean of $\boldsymbol{n}_D$ is zero and the covariance matrix $\boldsymbol{R}$ of $\boldsymbol{n}_D$ is given by

$$
\boldsymbol{R} = \sum_{k=1}^{K} \left( |\rho f_k|^2 \left( \boldsymbol{A}_k^H \boldsymbol{A}_k + \boldsymbol{B}_k^H \boldsymbol{B}_k \right) \right) + \boldsymbol{I}. \tag{7}
$$

Secondly, we present another system model, which is for the row-monomial DOSTBCs-CPI studied in Section IV. We assume that there is no strict power or size constraint on the relays and the relays can obtain partial CSI of the first hop by the equipped channel estimation devices. Specifically, we assume the $k$-th relay has the CPI of the first hop, i.e. it knows the phase $\theta_k$ of the channel coefficient $h_k$.[9] Note that this assumption does not imply more pilot signals compared to the assumption that relays have no CSI of the first hop. Actually, in order to make the destination have full CSI, the relays always need to forward the pilot signals from the source to the relays. Furthermore, the relays always need to transmit their own pilot signals to the destination. Therefore, the same amount of pilot signals is needed in all circumstances. Furthermore, the assumption that the relays have the CPI of the first hop does not imply any feedback overhead, because the relays do not need to have any CSI of the channels from themselves to the destination.

---

[8]We assume that there is no direct link between the source and destination. The same assumption has been made in many previous publications [21], [23], [24], [29]. Furthermore, perfect synchronization among the relays is assumed as in [20], [21], [23], and [27]–[29]. Although synchronization is a critical issue for the practical implementation of cooperative networks, it is beyond the scope of this paper.

[9]In this paper, we assume that the relays can estimate $\theta_k$ without any errors as in [27]–[29]. It will be interesting to study the scenario when the relays do not have perfect estimations of $\theta_k$; but it is beyond the scope of this paper.

Based on the CPI, the $k$-th relay first obtains $\boldsymbol{y}_k^C$ by $\boldsymbol{y}_k^C = e^{-j\theta_k}\boldsymbol{y}_k$ and then builds the transmitted signal vector $\boldsymbol{x}_k^C$ as

$$
\begin{aligned}
\boldsymbol{x}_k^C &= \rho(\boldsymbol{y}_k^C\boldsymbol{A}_k + \boldsymbol{y}_k^{C*}\boldsymbol{B}_k) \\
&= \rho|h_k|\boldsymbol{s}\boldsymbol{A}_k + \rho|h_k|\boldsymbol{s}^*\boldsymbol{B}_k + \rho e^{-j\theta_k}\boldsymbol{n}_k\boldsymbol{A}_k + \rho e^{j\theta_k}\boldsymbol{n}_k^*\boldsymbol{B}_k.
\end{aligned} \tag{8}
$$

Consequently, the received signal vector at the destination is given by

$$
\boldsymbol{y}_C = \boldsymbol{w}_C\boldsymbol{X}_C + \boldsymbol{n}_C, \tag{9}
$$

where

$$
\boldsymbol{w}_C = [\rho f_1|h_1|, \cdots, \rho f_K|h_K|] \tag{10}
$$

$$
\boldsymbol{X}_C = [\boldsymbol{s}\boldsymbol{A}_1 + \boldsymbol{s}^*\boldsymbol{B}_1; \cdots; \boldsymbol{s}\boldsymbol{A}_K + \boldsymbol{s}^*\boldsymbol{B}_K] \tag{11}
$$

$$
\boldsymbol{n}_C = \sum_{k=1}^{K}(\rho f_k e^{-j\theta_k}\boldsymbol{n}_k\boldsymbol{A}_k + \rho f_k e^{j\theta_k}\boldsymbol{n}_k^*\boldsymbol{B}_k) + \boldsymbol{n}_d. \tag{12}
$$

From (12), it is easy to see that the mean of $\boldsymbol{n}_C$ is zero and the covariance matrix $\boldsymbol{R}$ of $\boldsymbol{n}_C$ is still given by (7).

## III. DISTRIBUTED ORTHOGONAL SPACE-TIME BLOCK CODES

In this section, we abandon the row-monomial limitation, which was adopted in the construction of the row-monomial DOSTBCs in [1]. Thus, the codes possibly generate correlated noises at the destination. However, we still keep the CSI limitation, i.e. the relays do not have any CSI. It is easy to see that such codes are just the DOSTBCs proposed in [1], whose definition is as follows.

*Definition 1:* A $K \times T$ code matrix $\boldsymbol{X}_D$ is called a DOSTBC in variables $s_1, \cdots, s_N$ if the following two conditions are satisfied:

D1.1) The entries of $\boldsymbol{X}_D$ are $0$, $\pm h_k s_n$, $\pm h_k^* s_n^*$, or multiples of these indeterminates by $\mathbf{j}$, where $\mathbf{j} = \sqrt{-1}$.

D1.2) The matrix $\boldsymbol{X}_D$ satisfies the following equality

$$
\boldsymbol{X}_D\boldsymbol{R}^{-1}\boldsymbol{X}_D^H = |s_1|^2\boldsymbol{D}_1 + \cdots + |s_N|^2\boldsymbol{D}_N, \tag{13}
$$

where $\boldsymbol{D}_n = \mathrm{diag}[|h_1|^2 D_{n,1}, \cdots, |h_K|^2 D_{n,K}]$ and $D_{n,1}, \cdots, D_{n,K}$ are non-zero.

In [1], it has been shown the DOSTBCs are single-symbol ML decodable and achieve the full diversity order $K$. However, the bandwidth efficiency of the DOSTBCs has not been analyzed in [1]. Thus, it is still unknown if removing the row-monomial limitation can improve the bandwidth efficiency or not. In order to answer this question, we derive an upper bound of the data-rate of the DOSTBC in the following. To this end, one may think of redefining $\boldsymbol{w}_D$ and $\boldsymbol{X}_D$ as follows

$$
\boldsymbol{w}_D = [\rho f_1|h_1|, \cdots, \rho f_K|h_K|] \tag{14}
$$

$$
\boldsymbol{X}_D = [\boldsymbol{s}\tilde{\boldsymbol{A}}_1 + \boldsymbol{s}^*\tilde{\boldsymbol{B}}_1; \cdots; \boldsymbol{s}\tilde{\boldsymbol{A}}_K + \boldsymbol{s}^*\tilde{\boldsymbol{B}}_K], \tag{15}
$$

where $\tilde{A}_k = e^{j\theta_k} A_k$ and $\tilde{B}_k = e^{-j\theta_k} B_k$. Then $X_D$ can be seen as the generalized orthogonal designs, and hence, the results in [32] may be directly used. Actually, this method will make the analysis more complicated. Note that the new associated matrices $\tilde{A}_k$ and $\tilde{B}_k$ have a fundamental difference with the associated matrices of the generalized orthogonal design in [32]. That is, $\tilde{A}_k$ and $\tilde{B}_k$ contain $\theta_k$, which is a random variable. Due to this reason, it is very hard to find the properties of $\tilde{A}_k$ and $\tilde{B}_k$ by using the results in [32], and hence, it is very complicated to derive an upper bound by using (14) and (15). Instead of this approach, in this paper, we define $w_D$ and $X_D$ as in (3) and (4), respectively, and derive an upper bound of the data-rate by analyzing the properties of $A_k$ and $B_k$. Some fundamental properties of $A_k$ and $B_k$ are given in the following lemma at first.

*Lemma 1:* If a DOSTBC $X_D$ in variables $s_1, \cdots, s_N$ exists, its associated matrices $A_k$ and $B_k$ are column-monomial. Furthermore, the orthogonal condition (13) on $X_D$ holds if and only if

$$A_{k_1} R^{-1} A_{k_2}^H = 0, \qquad k_1 \neq k_2 \tag{16}$$

$$B_{k_1} R^{-1} B_{k_2}^H = 0, \qquad k_1 \neq k_2 \tag{17}$$

$$A_{k_1} R^{-1} B_{k_2}^H + B_{k_2}^* R^{-1} A_{k_1}^T = 0, \tag{18}$$

$$B_{k_1} R^{-1} A_{k_2}^H + A_{k_2}^* R^{-1} B_{k_1}^T = 0, \tag{19}$$

$$A_k R^{-1} A_k^H + B_k^* R^{-1} B_k^T = \mathrm{diag}[D_{1,k}, \cdots, D_{N,k}]. \tag{20}$$

*Proof:* By following the proof of Property 3.2 in [30], it is very easy to show that $A_k$ and $B_k$ are column-monomial. Furthermore, by following the proof of Lemma 1 in [1] and the proof of Proposition 1 in [32], it is not hard to show (16)–(20). □

Lemma 1 gives us some fundamental properties of $A_k$ and $B_k$. But, due to the existence of $R^{-1}$, we can not obtain an upper bound by using the conditions (16)–(20) directly. Therefore, we simplify those conditions in the following theorem by eliminating $R^{-1}$.

*Theorem 1:* If a DOSTBC $X_D$ in variables $s_1, \cdots, s_N$ exists, we have

$$X_D X_D^H = |s_1|^2 E_1 + \cdots + |s_N|^2 E_N, \tag{21}$$

where $E_n = \mathrm{diag}[|h_1|^2 E_{n,1}, \cdots, |h_K|^2 E_{n,K}]$ and $E_{n,1}, \cdots, E_{n,K}$ are strictly positive. Equivalently, the associated matrices $A_k$ and $B_k$ satisfy the following conditions

$$A_{k_1} A_{k_2}^H = 0, \qquad k_1 \neq k_2 \tag{22}$$

$$B_{k_1} B_{k_2}^H = 0, \qquad k_1 \neq k_2 \tag{23}$$

$$A_{k_1} B_{k_2}^H + B_{k_2}^* A_{k_1}^T = 0 \tag{24}$$

$$B_{k_1} A_{k_2}^H + A_{k_2}^* B_{k_1}^T = 0 \tag{25}$$

$$A_k A_k^H + B_k^* B_k^T = \mathrm{diag}[E_{1,k}, \cdots, E_{N,k}]. \tag{26}$$

*Proof:* See Appendix A. □

After comparing Theorem 1 and the definition of the generalized orthogonal design in [32], it seems that the DOSTBCs are in a subset of the generalized orthogonal design. However, note that there is a fundamental difference

between the DOSTBCs and the generalized orthogonal design. That is, the code matrix $\boldsymbol{X}_D$ of a DOSTBC contains the channel coefficients $h_k$. Actually, this fundamental difference explains why $\tilde{\boldsymbol{A}}_k$ and $\tilde{\boldsymbol{B}}_k$ in (15) contain $\theta_k$. Furthermore, this fundamental difference induces the conditions (22) and (23). Those two conditions help derive an upper bound of the data-rate of the DOSTBC in the following theorem.

*Theorem 2:* If a DOSTBC $\boldsymbol{X}_D$ in variables $s_1, \cdots, s_N$ exists, its data-rate $\mathcal{R}_D$ satisfies the following inequality:

$$\mathcal{R}_D = \frac{N}{T} \leq \frac{N}{\lceil \frac{NK}{2} \rceil}. \tag{27}$$

*Proof:* See Appendix B. □

Theorem 2 suggests that the DOSTBCs have approximately twice higher bandwidth efficiency than the repetition-based cooperative strategy. Furthermore, it is worthy of addressing that the DOSTBCs have the same decoding complexity and diversity order as the repetition-based cooperative strategy. On the other hand, when $N$ and $K$ are both even, the upper bound of the data-rate of the DOSTBC is exactly the same as that of the row-monomial DOSTBC proposed in [1]. Therefore, one can use the systematic construction method developed in Section V-A of [1] to build the DOSTBCs achieving the upper bound of (27) for this case. For the other cases when $N$ and/or $K$ are odd, the upper bound of the data-rate of the DOSTBC is larger than that of the row-monomial DOSTBC. Unfortunately, we have not found any DOSTBCs achieving the upper bound of (27) for those cases.

On the other hand, like the row-monomial DOSTBCs, the DOSTBCs may have poor bandwidth efficiency, when there are many relays. This is because the upper bound (27) decreases with the number $K$ of relays. This problem can be solved very well when the relays can exploit the CPI to construct the codes, which will be shown in the next section.

## IV. Row-Monomial Distributed Orthogonal Space-Time Block Codes with Channel Phase Information

In this section, we remove the CSI limitation and assume the relays use the CPI to construct the codes. But, we still keep the row-monomial limitation, in order to facilitate the analysis. Therefore, we define the row-monomial DOSTBCs-CPI in the following way.

*Definition 2:* A $K \times T$ code matrix $\boldsymbol{X}_C$ is called a row-monomial DOSTBC-CPI in variables $s_1, \cdots, s_N$ if it satisfies D1.1 in Definition 1 and the following equality

$$\boldsymbol{X}_C \boldsymbol{R}^{-1} \boldsymbol{X}_C^H = |s_1|^2 \boldsymbol{F}_1 + \cdots + |s_N|^2 \boldsymbol{F}_N, \tag{28}$$

where $\boldsymbol{F}_n = \text{diag}[F_{n,1}, \cdots, F_{n,K}]$ and $F_{n,1}, \cdots, F_{n,K}$ are non-zero. Furthermore, it associated matrices $\boldsymbol{A}_k$ and $\boldsymbol{B}_k$, $1 \leq k \leq K$, are all row-monomial.

It is easy to check that the row-monomial DOSTBCs-CPI are single-symbol ML decodable. By using the technique in [1] and [33], it can be shown that the row-monomial DOSTBCs-CPI also achieve the full diversity order. Furthermore, by following the proof of Lemma 1 and Theorem 1, it is not hard to show that a row-monomial

DOSTBC-CPI $\boldsymbol{X}_C$ satisfies the follow equality

$$\boldsymbol{X}_C \boldsymbol{X}_C^H \quad = \quad |s_1|^2 \boldsymbol{G}_1 + \cdots + |s_N|^2 \boldsymbol{G}_N, \tag{29}$$

where $\boldsymbol{G}_n = \mathrm{diag}[G_{n,1}, \cdots, G_{n,K}]$ and $G_{n,1}, \cdots, G_{n,K}$ are strictly positive. Note that the code matrix $\boldsymbol{X}_C$ of a row-monomial DOSTBC-CPI does not contain any channel coefficients. By comparing (29) and the definition of the generalized orthogonal design, we notice that a row-monomial DOSTBC-CPI must be a generalized orthogonal design. All the analysis of the generalized orthogonal design in [32] are valid for the row-monomial DOSTBCs-CPI. In particular, when $K = 2$, the data-rate of the row-monomial DOSTBC-CPI can be as large as one by using the Alamouti code proposed in [34]; when $K > 2$, the data-rate of the row-monomial DOSTBC-CPI is upper-bounded $4/5$, which is the upper bound of the data-rate of the generalized orthogonal design [32].

Actually, the row-monomial DOSTBCs-CPI have some unique properties which the generalized orthogonal design does not have. Those unique properties help find a tighter upper bound of the data-rate of the row-monomial DOSTBC-CPI. To this end, we first have the following theorem.

*Theorem 3:* Assume $\boldsymbol{X}_C$ is a DSTC in variables $s_1, \cdots, s_N$, i.e. every row of $\boldsymbol{X}_C$ contains the information-bearing symbols $s_1, \cdots, s_N$. Moreover, assume that the noise covariance matrix $\boldsymbol{R}$ of $\boldsymbol{X}_C$ is diagonal. After proper column permutations, we can partition $\boldsymbol{R}^{-1}$ into $\boldsymbol{R}^{-1} = \mathrm{diag}[\boldsymbol{R}_1, \boldsymbol{R}_2, \cdots, \boldsymbol{R}_W]$ such that the main diagonal entries of $\boldsymbol{R}_w$ are all equal to $R_w$ and $R_i \neq R_j$ for $i \neq j$. After the same column permutations, we can partition $\boldsymbol{X}_C$ into $\boldsymbol{X}_C = [\boldsymbol{X}_{C1}, \cdots, \boldsymbol{X}_{CW}]$. Let $\tilde{\boldsymbol{X}}_{Cw}$ denote all the non-zero rows in $\boldsymbol{X}_{Cw}$. Assume that $\tilde{\boldsymbol{X}}_{Cw}$ contains $N_w$ different information-bearing symbols and they are $s_1^w, \cdots, s_{N_w}^w$.[10] Then $\boldsymbol{X}_C$ is a row-monomial DOSTBC-CPI if and only if every sub-matrix $\tilde{\boldsymbol{X}}_{Cw}$ is a row-monomial DOSTBC-CPI in variables $s_1^w, \cdots, s_{N_w}^w$.

*Proof:* See Appendix C. □

Theorem 3 means that, when a DSTC $\boldsymbol{X}_C$ generates uncorrelated noises at the destination, the code is single-symbol ML decodable as long as it can be partitioned into several single-symbol ML decodable codes.[11] Furthermore, Theorem 3 is crucial to derive an upper bound of the data-rate of the row-monomial DOSTBC-CPI. This is because it enables us to analyze the data-rate of every individual sub-matrix $\tilde{\boldsymbol{X}}_{Cw}$ instead of $\boldsymbol{X}_C$ itself. When $\tilde{\boldsymbol{X}}_{Cw}$ has one or two rows, it is easy to see that its data-rate can be as large as one. When $\tilde{\boldsymbol{X}}_{Cw}$ has more than two rows, the following theorem shows that the data-rate of $\tilde{\boldsymbol{X}}_{Cw}$ is exactly $1/2$.

*Theorem 4:* Assume $\boldsymbol{X}_C$ is a row-monomial DOSTBC-CPI and its noise covariance matrix is $\boldsymbol{R}$. By proper column permutations, we can partition $\boldsymbol{R}^{-1}$ into $\boldsymbol{R}^{-1} = \mathrm{diag}[\boldsymbol{R}_1, \boldsymbol{R}_2, \cdots, \boldsymbol{R}_W]$ such that the main diagonal entries of $\boldsymbol{R}_w$ are all equal to $R_w$ and $R_i \neq R_j$ for $i \neq j$. By the same column permutations, we can partition $\boldsymbol{X}_C$ into $\boldsymbol{X}_C = [\boldsymbol{X}_{C1}, \cdots, \boldsymbol{X}_{CW}]$. Let $\tilde{\boldsymbol{X}}_{Cw}$ denote all the non-zero rows in $\boldsymbol{X}_{Cw}$ and assume the dimension of

---

[10]Note that $s_1^w, \cdots, s_{N_w}^w$ are all from the set $\boldsymbol{s} = [s_1, \cdots, s_N]$.

[11]For the rate-3/4 code in [29], it generates uncorrelated noises at the destination; but the main diagonal entries of $\boldsymbol{R}$ are all different. If we partition the rate-3/4 code by the way presented in Theorem 3, we will see that every sub-matrix $\tilde{\boldsymbol{X}}_{Cw}$ is actually a column vector with more than one non-zero entries. Thus, $\tilde{\boldsymbol{X}}_{Cw}$ can not be a row-monomial DOSTBC-CPI, and hence, it is not single-symbol ML decodable. By Theorem 3, the rate-3/4 code can not be a row-monomial DOSTBC-CPI either and it is not single-symbol ML decodable.

$\tilde{\boldsymbol{X}}_{Cw}$ is $K_w \times T_w$. Then the data-rate of $\tilde{\boldsymbol{X}}_{Cw}$ is exactly $1/2$ when $K_w > 2$.

*Proof:* See Appendix D. □

Based on Theorems 3 and 4, we derive an upper bound of the data-rate of the row-monomial DOSTBC-CPI in the following theorem.

*Theorem 5:* When $K > 2$, the data-rate $\mathcal{R}_C$ of the row-monomial DOSTBC-CPI satisfies the following inequality

$$\mathcal{R}_C = \frac{N}{T} \leq \frac{1}{2}. \tag{30}$$

*Proof:* See Appendix E. □

We notice that the data-rate of the row-monomial DOSTBC-CPI is independent of the number $K$ of relays. Thus, the row-monomial DOSTBCs-CPI have good bandwidth efficiency even in a cooperative network with many relays. Furthermore, compared to the row-monomial DOSTBCs and the DOSTBCs, the row-monomial DOSTBCs-CPI improve bandwidth efficiency considerably, especially when the cooperative network has a large number of relays. The improvement is mainly because the relays exploit the CPI to construct the codes. As we have seen, because the code matrix $\boldsymbol{X}_D$ of a DOSTBC contains the channel coefficient $h_k$, the conditions (22) and (23) are induced. Those two conditions severely constrain the data-rate of the DOSTBC. On the other hand, by exploiting the CPI, the code matrix $\boldsymbol{X}_C$ of a row-monomial DOSTBC-CPI does not have any channel coefficients. Thus, the conditions (22) and (23) are not induced, and the data-rate is greatly improved. Furthermore, recall that exploiting the CPI at the relays does not increase the pilot signals or require any feedback overhead. Compared to the DOSTBCs, the only extra cost of the row-monomial DOSTBCs-CPI is that the relays should be equipped with some channel estimation devices to estimate $\theta_k$.

Interestingly, the row-monomial DOSTBCs-CPI achieving the upper bound $1/2$ are easy to construct and they are given in the following theorem.

*Theorem 6:* The rate-halving codes developed in [31] can be used as the row-monomial DOSTBCs-CPI achieving the upper bound $1/2$ of the data-rate.

*Proof:* It is easy to check that the rate-halving codes satisfy Definition 2 and they always achieve the data-rate $1/2$. □

As an example, when $N = 4$ and $K = 4$, the row-monomial DOSTBC-CPI achieving the upper bound $1/2$ is given as follows:

$$\boldsymbol{X}_C = \begin{bmatrix} s_1 & -s_2 & -s_3 & -s_4 & s_1^* & -s_2^* & -s_3^* & -s_4^* \\ s_2 & s_1 & s_4 & -s_3 & s_2^* & s_1^* & s_4^* & -s_3^* \\ s_3 & -s_4 & s_1 & s_2 & s_3^* & -s_4^* & s_1^* & s_2^* \\ s_4 & s_3 & -s_2 & s_1 & s_4^* & s_3^* & -s_2^* & s_1^* \end{bmatrix}. \tag{31}$$

## V. NUMERICAL RESULTS

In this section, we present some numerical results to demonstrate the performance of the DOSTBCs and the row-monomial DOSTBCs-CPI. In our simulation, we define the average signal to noise ratio (SNR) per bit as the

ratio of $E_r$ to the logarithm of the size of the modulation scheme. Furthermore, we adopt the power allocation proposed in [23], i.e. $E_s = KE_r$.

In Fig. 1, we let $N = 4$ and $K = 4$. For this case, we see that the average bit error rate (BER) performance of the DOSTBCs and the row-monomial DOSTBCs-CPI is much better than that of the repetition-based cooperative strategy, especially when the bandwidth efficiency is 2 bps/Hz. The DOSTBCs and the row-monomial DOSTBCs-CPI have almost the same performance. This is because, when $N = 4$ and $K = 4$, the DOSTBCs and the row-monomial DOSTBCs-CPI have the same data-rate $1/2$. Fig. 1 also demonstrates that the performance of the DOSTBCs and the row-monomial DOSTBCs-CPI is slightly worse than that of the rate-$3/4$ code proposed in [29]. But, note that the rate-$3/4$ code is not single-symbol ML decodable, and hence, its decoding complexity is much higher than that of the DOSTBCs and the row-monomial DOSTBCs-CPI. In Fig. 2, we set $N = 8$ and $K = 6$. For this case, the average BER performance of the row-monomial DOSTBCs-CPI is now much better than that of the DOSTBCs. This is because, when $N = 8$ and $K = 6$, the data-rate of the row-monomial DOSTBC-CPI is still $1/2$; while the data-rate of the DOSTBC becomes $1/3$.

## VI. CONCLUSION AND FUTURE WORK

In the first part of this paper, we consider the DOSTBCs, where the noises at the destination are possibly correlated and the relays have no CSI of the first hop. An upper bound of the data-rate of the DOSTBC is derived. When $N$ and $K$ are both even, the upper bond of the data-rate of the DOSTBC is exactly the same as that of the row-monomial DOSTBC in [1]. When $N$ and/or $K$ are odd, the upper bound of the data-rate of the DOSTBC is larger than that of the row-monomial DOSTBC, which means the DOSTBCs can potentially improve the bandwidth efficiency. However, we notice that, like the row-monomial DOSTBCs, the DOSTBCs may not have good bandwidth efficiency in a cooperative network with many relays, because the upper-bound of the data-rate of the DOSTBC decreases with the number $K$ of the relays. In the second part of this paper, we propose the row-monomial DOSTBCs-CPI, where the noises at the destination are always uncorrelated and the relays exploit the CPI of the first hop to construct the codes. We derive an upper bound of the data-rate of those codes and find the actual codes achieving this upper bound. The upper bound of the data-rate of the row-monomial DOSTBC-CPI suggests that the row-monomial DOSTBCs-CPI have better bandwidth efficiency than the DOSTBCs and the row-monomial DOSTBCs. Moreover, the upper bound of the data-rate of the row-monomial DOSTBC-CPI is independent of the number $K$ of the relays, and hence, the codes have good bandwidth efficiency even in a cooperative network with many relays.

Our work can be extended in the following two ways. First, it will be very interesting to consider a more general case, where the noises at the destination are possibly correlated and the relays use the CPI of the first hop to construct the codes. Intuitively, such codes should have even higher data-rate than the row-monomial DOSTBCs-CPI. But, we conjecture that the improvement of the data-rate is just marginal. This is because, by comparing the DOSTBCs and the row-monomial DOSTBCs, we notice that removing the row-monomial limitation just slightly improves the data-rate. Secondly, we can assume that the relays have the full CSI, including not only the channel phase $\theta_k$ but also the channel magnitude $|h_k|$, of the first hop and use this information in the code construction.

We notice that the use of the channel magnitude $|h_k|$ only affects the structure of the noise covariance matrix $\boldsymbol{R}$; but it can not change the structure of the code matrix $\boldsymbol{X}_C$. Therefore, we conjecture that the data-rate can not be improved by assuming the relays have the full CSI of the first hop.

## APPENDIX A

### Proof of Theorem 1

By following the proof of Lemma 1, it can be easily shown that (21) is equivalent with the conditions (22)–(26). On the other hand, if a DOSTBC $\boldsymbol{X}_D$ exists, (13) holds by Definition 1, and hence, (16)–(20) hold by Lemma 1. Therefore, in order to prove Theorem 1, we only need to show that, if (16)–(20) hold, (22)–(26) hold and $E_{n,k}$ is strictly positive.

We start our proof by evaluating $[\boldsymbol{R}]_{t_1,t_2}$ and $[\boldsymbol{R}^{-1}]_{t_1,t_2}$. According to (7), when $t_1 \neq t_2$, $[\boldsymbol{R}]_{t_1,t_2}$ can be either null or a sum of several terms containing $|\rho f_k|^2$; when $t_1 = t_2 = t$, $[\boldsymbol{R}]_{t,t}$ is a sum of a constant 1, which is from the identity matrix, and several terms containing $|\rho f_k|^2$. Therefore, we can rewrite $[\boldsymbol{R}]_{t,t}$ as $[\boldsymbol{R}]_{t,t} = \bar{R}_{t,t} + 1$, where $\bar{R}_{t,t}$ accounts for all the terms containing $|\rho f_k|^2$. $[\boldsymbol{R}^{-1}]_{t_1,t_2}$ is given by $[\boldsymbol{R}^{-1}]_{t_1,t_2} = C_{t_2,t_1}/\det(\boldsymbol{R})$, where $C_{t_2,t_1}$ is the matrix cofactor of $[\boldsymbol{R}]_{t_2,t_1}$. When $t_1 = t_2 = t$, by the definition of matrix cofactor, $C_{t,t}$ contains a constant 1 generated by the product $\prod_{i=1,i\neq t}^{T}[\boldsymbol{R}]_{i,i} = \prod_{i=1,i\neq t}^{T}(\bar{R}_{i,i} + 1)$. Furthermore, it is easy to see that the constant 1 is the only constant term in $C_{t,t}$. Thus, $C_{t,t}$ can be rewritten as $C_{t,t} = \bar{C}_{t,t} + 1$ and there is no constant term in $\bar{C}_{t,t}$. Consequently, $[\boldsymbol{R}^{-1}]_{t,t}$ can be rewritten as $[\boldsymbol{R}^{-1}]_{t,t} = \bar{C}_{t,t}/\det(\boldsymbol{R}) + 1/\det(\boldsymbol{R})$. When $t_1 \neq t_2$, $C_{t_2,t_1}$ does not contain any constant term, and hence, $[\boldsymbol{R}^{-1}]_{t_1,t_2}$ does not contain the term $1/\det(\boldsymbol{R})$.[12] Therefore, we can extract the term $1/\det(\boldsymbol{R})$ from every main diagonal entry of $\boldsymbol{R}^{-1}$ and rewrite $\boldsymbol{R}^{-1}$ in the following way

$$\boldsymbol{R}^{-1} = \frac{1}{\det(\boldsymbol{R})}\bar{\boldsymbol{C}} + \frac{1}{\det(\boldsymbol{R})}\boldsymbol{I}. \tag{A.1}$$

Then we show that (22) holds if (16) holds. If (16) holds, we have

$$\boldsymbol{A}_{k_1}\boldsymbol{R}^{-1}\boldsymbol{A}_{k_2}^H = \frac{1}{\det(\boldsymbol{R})}\boldsymbol{A}_{k_1}\bar{\boldsymbol{C}}\boldsymbol{A}_{k_2}^H + \frac{1}{\det(\boldsymbol{R})}\boldsymbol{A}_{k_1}\boldsymbol{A}_{k_2}^H = \boldsymbol{0}. \tag{A.2}$$

Note that $\boldsymbol{R}^{-1}$ and $\bar{\boldsymbol{C}}$ are random matrices. In order to make (A.2) hold for every possible $\boldsymbol{R}^{-1}$ and $\bar{\boldsymbol{C}}$, both terms in (A.2) must be equal to zero. Therefore, (22) holds. Similarly, we can show that (23)–(25) hold if (17)–(19) hold. Now, we show that (26) holds if (20) holds. If (20) holds, we have

$$\begin{aligned} \boldsymbol{A}_k\boldsymbol{R}^{-1}\boldsymbol{A}_k^H + \boldsymbol{B}_k^*\boldsymbol{R}^{-1}\boldsymbol{B}_k^T &= \frac{1}{\det(\boldsymbol{R})}\left(\boldsymbol{A}_k\bar{\boldsymbol{C}}\boldsymbol{A}_k^H + \boldsymbol{B}_k^*\bar{\boldsymbol{C}}\boldsymbol{B}_k^T\right) + \frac{1}{\det(\boldsymbol{R})}\left(\boldsymbol{A}_k\boldsymbol{A}_k^H + \boldsymbol{B}_k^*\boldsymbol{B}_k^T\right) \\ &= \mathrm{diag}[D_{1,k}, \cdots, D_{N,k}]. \end{aligned} \tag{A.3}$$

For the same reason as in (A.2), the off-diagonal entries of $\boldsymbol{A}_k\boldsymbol{A}_k^H + \boldsymbol{B}_k^*\boldsymbol{B}_k^T$ must be zero, and hence, (26) holds.

---

[12]$C_{t_2,t_1}$ may be zero; but it does not change the conclusion that $[\boldsymbol{R}^{-1}]_{t_1,t_2}$ does not contain the term $1/\det(\boldsymbol{R})$.

Lastly, we show that $E_{n,k}$ is strictly positive if (20) holds. From (20) and (26), we have

$$
D_{n,k} = \sum_{t=1}^{T}\sum_{i=1}^{T}[\boldsymbol{R}^{-1}]_{i,t}([\boldsymbol{A}_k]_{n,i}[\boldsymbol{A}_k]_{n,t}^* + [\boldsymbol{B}_k]_{n,i}^*[\boldsymbol{B}_k]_{n,t}) \tag{A.4}
$$

$$
E_{n,k} = \sum_{t=1}^{T}(|[\boldsymbol{A}_k]_{n,t}|^2 + |[\boldsymbol{B}_k]_{n,t}|^2). \tag{A.5}
$$

Since $D_{n,k}$ is non-zero, at least one $[\boldsymbol{A}_k]_{n,t}$ or one $[\boldsymbol{B}_k]_{n,t}$ is non-zero. Therefore, $E_{n,k} = \sum_{t=1}^{T}(|[\boldsymbol{A}_k]_{n,t}|^2 + |[\boldsymbol{B}_k]_{n,t}|^2)$ is strictly positive, which completes the proof of Theorem 1.

## APPENDIX B

## Proof of Theorem 2

Let $\underline{\boldsymbol{A}} = [\boldsymbol{A}_1, \cdots, \boldsymbol{A}_K]^T$ and $\underline{\boldsymbol{B}} = [\boldsymbol{B}_1, \cdots, \boldsymbol{B}_K]^T$; then the dimension of $\underline{\boldsymbol{A}}$ and $\underline{\boldsymbol{B}}$ is $NK \times T$. From (22), every row of $\boldsymbol{A}_{k_1}$ is orthogonal with every row of $\boldsymbol{A}_{k_2}$ when $k_1 \neq k_2$.[13] Furthermore, because $\boldsymbol{A}_k$ is column-monomial by Lemma 1, every row of $\boldsymbol{A}_k$ is orthogonal with every other row of $\boldsymbol{A}_k$. Therefore, any two different rows in $\underline{\boldsymbol{A}}$ are orthogonal with each other, and hence, $\mathrm{rank}(\underline{\boldsymbol{A}}) = \sum_{k=1}^{K}\mathrm{rank}(\boldsymbol{A}_k)$. Similarly, any two different rows in $\underline{\boldsymbol{B}}$ are orthogonal with each other, and hence, $\mathrm{rank}(\underline{\boldsymbol{B}}) = \sum_{k=1}^{K}\mathrm{rank}(\boldsymbol{B}_k)$.

On the other hand, from (26), we have

$$
\mathrm{rank}(\boldsymbol{A}_k) + \mathrm{rank}(\boldsymbol{B}_k) \geq \mathrm{rank}(\mathrm{diag}[E_{1,k}, \cdots, E_{N,k}]) = N, \tag{B.1}
$$

where the inequality is from the rank inequality 3) in [32], and hence,

$$
\sum_{k=1}^{K}\mathrm{rank}(\boldsymbol{A}_k) + \sum_{k=1}^{K}\mathrm{rank}(\boldsymbol{B}_k) \geq NK. \tag{B.2}
$$

Because $\mathrm{rank}(\underline{\boldsymbol{A}})$ and $\mathrm{rank}(\underline{\boldsymbol{B}})$ are integers, we have

$$
\mathrm{rank}(\underline{\boldsymbol{A}}) = \sum_{k=1}^{K}\mathrm{rank}(\boldsymbol{A}_k) \geq \left\lceil \frac{NK}{2} \right\rceil \tag{B.3}
$$

or

$$
\mathrm{rank}(\underline{\boldsymbol{B}}) = \sum_{k=1}^{K}\mathrm{rank}(\boldsymbol{B}_k) \geq \left\lceil \frac{NK}{2} \right\rceil. \tag{B.4}
$$

If (B.3) is true, $T \geq \mathrm{rank}(\underline{\boldsymbol{A}}) \geq \lceil (NK)/2 \rceil$ and (27) holds. If (B.4) is true, the same conclusion can be made.

## APPENDIX C

## Proof of Theorem 3

The sufficient part is easy to verify. Thus, we focus on the necessary part, i.e. if $\boldsymbol{X}_C$ is a row-monomial DOSTBC-CPI, all the sub-matrices $\tilde{\boldsymbol{X}}_{Cw}$ are also row-monomial DOSTBCs-CPI. Assume that the dimension of $\boldsymbol{R}_w$ is $T_w \times T_w$.

---

[13]A row vector $\boldsymbol{x}$ is said to be orthogonal with another row vector $\boldsymbol{y}$ if $\boldsymbol{x}\boldsymbol{y}^H$ is equal to zero.

Firstly, we show that $\tilde{\boldsymbol{X}}_{Cw}\boldsymbol{R}_w\tilde{\boldsymbol{X}}_{Cw}^H$ is a diagonal matrix. Based on (28), when $k_1 \neq k_2$, $[\boldsymbol{X}_C\boldsymbol{R}^{-1}\boldsymbol{X}_C^H]_{k_1,k_2}$ is given by

$$[\boldsymbol{X}_C\boldsymbol{R}^{-1}\boldsymbol{X}_C^H]_{k_1,k_2} = \sum_{w=1}^{W}\sum_{t=1}^{T_w}[\boldsymbol{X}_{Cw}]_{k_1,t}[\boldsymbol{X}_{Cw}]_{k_2,t}^*R_w = 0. \tag{C.1}$$

If all the terms in this summation are zero, it is trivial to show that $\sum_{t=1}^{T_w}[\boldsymbol{X}_{Cw}]_{k_1,t}[\boldsymbol{X}_{Cw}]_{k_2,t}^*R_w = 0$ for $1 \leq w \leq W$. Because $\tilde{\boldsymbol{X}}_{Cw}$ contains all the non-zero entries of $\boldsymbol{X}_{Cw}$, we have $[\tilde{\boldsymbol{X}}_{Cw}\boldsymbol{R}_w\tilde{\boldsymbol{X}}_{Cw}^H]_{k_1,k_2} = [\boldsymbol{X}_{Cw}\boldsymbol{R}_w\boldsymbol{X}_{Cw}^H]_{k_1,k_2} = \sum_{t=1}^{T_w}[\boldsymbol{X}_{Cw}]_{k_1,t}[\boldsymbol{X}_{Cw}]_{k_2,t}^*R_w = 0$, which means $\tilde{\boldsymbol{X}}_{Cw}\boldsymbol{R}_w\tilde{\boldsymbol{X}}_{Cw}^H$ is a diagonal matrix.

If there is one term $[\boldsymbol{X}_{Cw_1}]_{k_1,t_1}[\boldsymbol{X}_{Cw_1}]_{k_2,t_1}^*R_{w_1} \neq 0$, some other terms must cancel this term in order to make (C.1) hold. Actually, the non-zero term $[\boldsymbol{X}_{Cw_1}]_{k_1,t_1}[\boldsymbol{X}_{Cw_1}]_{k_2,t_1}^*R_{w_1}$ must be cancelled by exactly one other term. This can be shown by contradiction. We assume that $[\boldsymbol{X}_{Cw_1}]_{k_1,t_1}[\boldsymbol{X}_{Cw_1}]_{k_2,t_1}^*R_{w_1}$ is cancelled by two other terms together, i.e.

$$[\boldsymbol{X}_{Cw_1}]_{k_1,t_1}[\boldsymbol{X}_{Cw_1}]_{k_2,t_1}^*R_{w_1} + [\boldsymbol{X}_{Cw_2}]_{k_1,t_2}[\boldsymbol{X}_{Cw_2}]_{k_2,t_2}^*R_{w_2} + [\boldsymbol{X}_{Cw_3}]_{k_1,t_3}[\boldsymbol{X}_{Cw_3}]_{k_2,t_3}^*R_{w_3} = 0. \tag{C.2}$$

In order to make this equality hold, one of the following three equalities must hold: 1) $[\boldsymbol{X}_{Cw_2}]_{k_1,t_2} = \pm[\boldsymbol{X}_{Cw_1}]_{k_1,t_1}$; 2) $[\boldsymbol{X}_{Cw_3}]_{k_1,t_3} = \pm[\boldsymbol{X}_{Cw_1}]_{k_1,t_1}$; 3) $\pm[\boldsymbol{X}_{Cw_2}]_{k_1,t_2} = \pm[\boldsymbol{X}_{Cw_3}]_{k_1,t_3} = [\boldsymbol{X}_{Cw_1}]_{k_2,t_1}^*$. However, those three equalities all contradict with our assumption that the covariance matrix $\boldsymbol{R}$ is diagonal. For example, we assume $[\boldsymbol{X}_{Cw_1}]_{k_1,t_1} = s_n^{w_1}$, $1 \leq n \leq N_{w_1}$, and the equality $[\boldsymbol{X}_{Cw_2}]_{k_1,t_2} = \pm[\boldsymbol{X}_{Cw_1}]_{k_1,t_1}$ holds. Thus, $[\boldsymbol{X}_{Cw_2}]_{k_1,t_2} = \pm s_n^{w_1}$ and $s_n^{w_1}$ is transmitted in the $k_1$-th row of $\boldsymbol{X}_C$ for at least twice. This makes the noise covariance matrix $\boldsymbol{R}$ non-diagonal, which contradicts with our assumption. If we assume $[\boldsymbol{X}_{Cw_1}]_{k_1,t_1}[\boldsymbol{X}_{Cw_1}]_{k_2,t_1}^*R_{w_1}$ is cancelled by more than two other terms, the same contradiction can be seen similarly. Thus, $[\boldsymbol{X}_{Cw_1}]_{k_1,t_1}[\boldsymbol{X}_{Cw_1}]_{k_2,t_1}^*R_{w_1}$ is cancelled by exactly one other term in the summation (C.1) and we have

$$[\boldsymbol{X}_{Cw_1}]_{k_1,t_1}[\boldsymbol{X}_{Cw_1}]_{k_2,t_1}^*R_{w_1} + [\boldsymbol{X}_{Cw_2}]_{k_1,t_2}[\boldsymbol{X}_{Cw_2}]_{k_2,t_2}^*R_{w_2} = 0. \tag{C.3}$$

Furthermore, because $R_i \neq R_j$ when $i \neq j$, (C.3) also implies that $R_{w_1} = R_{w_2}$ and $w_1 = w_2$. This means that, if one term in the summation (C.1) is non-zero, it must be cancelled by exactly one other term, which is from the same sub-matrix $\boldsymbol{X}_{Cw}$. Therefore, we have $\sum_{t=1}^{T_w}[\boldsymbol{X}_{Cw}]_{k_1,t}[\boldsymbol{X}_{Cw}]_{k_2,t}^*R_w = 0$ when $k_1 \neq k_2$. Because $\tilde{\boldsymbol{X}}_{Cw}$ contains all the non-zero entries of $\boldsymbol{X}_{Cw}$, we have $[\tilde{\boldsymbol{X}}_{Cw}\boldsymbol{R}_w\tilde{\boldsymbol{X}}_{Cw}^H]_{k_1,k_2} = [\boldsymbol{X}_{Cw}\boldsymbol{R}_w\boldsymbol{X}_{Cw}^H]_{k_1,k_2} = \sum_{t=1}^{T_w}[\boldsymbol{X}_{Cw}]_{k_1,t}[\boldsymbol{X}_{Cw}]_{k_2,t}^*R_w = 0$, when $k_1 \neq k_2$. Therefore, $\tilde{\boldsymbol{X}}_{Cw}\boldsymbol{R}_w\tilde{\boldsymbol{X}}_{Cw}^H$ is a diagonal matrix.

Secondly, we show that the information-bearing symbols $s_1^w, \cdots, s_{N_w}^w$ are contained in every row of $\tilde{\boldsymbol{X}}_{Cw}$. Because every main diagonal entry of $\boldsymbol{R}_w$ is the same, it follows from (7) that every column in $\boldsymbol{X}_{Cw}$ has non-zero entries at the same rows. Therefore, the non-zero rows in $\boldsymbol{X}_{Cw}$ does not contain any zero entries. Since $\tilde{\boldsymbol{X}}_{Cw}$ contains all the non-zero rows in $\boldsymbol{X}_{Cw}$, every entry in $\tilde{\boldsymbol{X}}_{Cw}$ is non-zero. Then we assume that $[\tilde{\boldsymbol{X}}_{Cw}]_{k_1,t_1} = s_n^w$, $1 \leq n \leq N_w$. Because every entry in $\tilde{\boldsymbol{X}}_{Cw}$ is non-zero, we can find another non-zero entry $[\tilde{\boldsymbol{X}}_{Cw}]_{k_2,t_1}$, $k_1 \neq k_2$, from the $t_1$-th column of $\tilde{\boldsymbol{X}}_{Cw}$. Thus, $[\tilde{\boldsymbol{X}}_{Cw}\boldsymbol{R}_w\tilde{\boldsymbol{X}}_{Cw}^H]_{k_1,k_2}$ must contain the term $[\tilde{\boldsymbol{X}}_{Cw}]_{k_1,t_1}[\tilde{\boldsymbol{X}}_{Cw}]_{k_2,t_1}^*R_w$. Because $[\tilde{\boldsymbol{X}}_{Cw}\boldsymbol{R}_w\tilde{\boldsymbol{X}}_{Cw}^H]_{k_1,k_2} = 0$, $[\tilde{\boldsymbol{X}}_{Cw}]_{k_1,t_1}[\tilde{\boldsymbol{X}}_{Cw}]_{k_2,t_1}^*R_w$ must be cancelled by another term and we assume it is $[\tilde{\boldsymbol{X}}_{Cw}]_{k_1,t_2}[\tilde{\boldsymbol{X}}_{Cw}]_{k_2,t_2}^*R_w$, $t_1 \neq t_2$. In order to make $[\tilde{\boldsymbol{X}}_{Cw}]_{k_1,t_1}[\tilde{\boldsymbol{X}}_{Cw}]_{k_2,t_1}^*R_w + [\tilde{\boldsymbol{X}}_{Cw}]_{k_1,t_2}[\tilde{\boldsymbol{X}}_{Cw}]_{k_2,t_2}^*R_w = 0$, we must have $[\tilde{\boldsymbol{X}}_{Cw}]_{k_1,t_2} = \pm[\tilde{\boldsymbol{X}}_{Cw}]_{k_1,t_1}$ or $[\tilde{\boldsymbol{X}}_{Cw}]_{k_2,t_2}^* = \pm[\tilde{\boldsymbol{X}}_{Cw}]_{k_1,t_1}$. Due to the row-monomial condition,

$[\tilde{\boldsymbol{X}}_{Cw}]_{k_1,t_2}$ can not be $\pm[\tilde{\boldsymbol{X}}_{Cw}]_{k_1,t_1}$, and hence, we have $[\tilde{\boldsymbol{X}}_{Cw}]_{k_2,t_2} = \pm[\tilde{\boldsymbol{X}}_{Cw}]_{k_1,t_1}^* = \pm s_n^{w*}$. This means that the $k_2$-th row contains the information-bearing symbol $s_n^w$ as well. Taking a similar approach, we can show that the information-bearing symbols $s_1^w, \cdots, s_{N_w}^w$ are contained in every row of $\tilde{\boldsymbol{X}}_{Cw}$.

Because $\tilde{\boldsymbol{X}}_{Cw}\boldsymbol{R}_w\tilde{\boldsymbol{X}}_{Cw}^H$ is a diagonal matrix and every row of $\tilde{\boldsymbol{X}}_{Cw}$ contains all the information-bearing symbols $s_1^w, \cdots, s_{N_w}^w$, $\tilde{\boldsymbol{X}}_{Cw}\boldsymbol{R}_w\tilde{\boldsymbol{X}}_{Cw}^H$ can be written as

$$\tilde{\boldsymbol{X}}_{Cw}\boldsymbol{R}_w\tilde{\boldsymbol{X}}_{Cw}^H = |s_1^w|^2\boldsymbol{M}_1 + \cdots + |s_{N_w}^w|^2\boldsymbol{M}_{N_w}, \tag{C.4}$$

where $\boldsymbol{M}_n$ are diagonal and all the main diagonal entries are non-zero. Note that, if the relays only transmit $\tilde{\boldsymbol{X}}_{Cw}$ to the destination, $\boldsymbol{R}_w$ is actually the inverse of the noise covariance matrix at the destination. This is because $\tilde{\boldsymbol{X}}_{Cw}$ and $\boldsymbol{R}_w$ are obtained after the same column permutations. Therefore, (C.4) is equivalent with (28). Furthermore, since $\tilde{\boldsymbol{X}}_{Cw}$ is a sub-matrix of $\boldsymbol{X}_C$, it automatically satisfies D1.1 and the row-monomial condition. Thus, we conclude that $\tilde{\boldsymbol{X}}_{Cw}$ satisfies Definition 2 and it is a row-monomial DOSTBC-CPI.

## APPENDIX D

## Proof of Theorem 4

From Theorem 3, every sub-matrix $\tilde{\boldsymbol{X}}_{Cw}$ is a row-monomial DOSTBC-CPI in variables $s_1^w, \cdots, s_{N_w}^w$. Furthermore, by (29), every sub-matrix $\tilde{\boldsymbol{X}}_{Cw}$ is also a generalized orthogonal design. For convenience, we refer to any entry containing $s_{n_w}^w$ as the $s_{n_w}^w$-entry. Similarly, any entry containing $s_{n_w}^{w*}$ is referred to as the $s_{n_w}^{w*}$-entry.

By the row-monomial condition, any row in $\tilde{\boldsymbol{X}}_{Cw}$ can not contain more than one $s_{n_w}^w$-entry or $s_{n_w}^{w*}$-entry. Therefore, the data-rate of $\tilde{\boldsymbol{X}}_{Cw}$ is lower-bounded by $1/2$, which is achieved when every row contains exactly one $s_{n_w}^w$-entry and one $s_{n_w}^{w*}$-entry for $1 \leq n_w \leq N_w$.

Then we show that the data-rate can not be strictly larger than $1/2$ by contradiction. Without loss of generality, we assume the first row of $\tilde{\boldsymbol{X}}_{Cw}$ is $[s_1^w, \cdots, s_{N_w}^w, s_1^{w*}, \cdots, s_{N_w'}^{w*}]$, where $N_w' < N_w$. Hence, the data-rate of $\tilde{\boldsymbol{X}}_{Cw}$ is $N_w/(N_w + N_w')$ and it is strictly larger than $1/2$. Furthermore, because every entry in $\tilde{\boldsymbol{X}}_{Cw}$ is non-zero, this assumption also means that every row in $\tilde{\boldsymbol{X}}_{Cw}$ contains exactly $N_w + N_w'$ non-zero entries. Because $s_{N_w'+1}^{w*}, \cdots, s_{N_w}^{w*}$ are not transmitted by the first row, the second row can not have any $s_{n_w}^w$-entries, $N_w' + 1 \leq n_w \leq N_w$. This can be shown by contradiction. For example, if the second row has $s_{N_w'+1}^w$ on the first column, the inner product of the first and second rows must have the term $s_1^w s_{N_w'+1}^{w*}$. Because $\tilde{\boldsymbol{X}}_{Cw}$ is a generalized orthogonal design, the inner product of any two rows must be zero. In order to cancel the term $s_1^w s_{N_w'+1}^{w*}$, the first row must have an $s_{N_w'+1}^{w*}$-entry, which contradicts our assumption. Thus, the second row can not contain any $s_{n_w}^w$-entries, $N_w' + 1 \leq n_w \leq N_w$. On the other hand, because the second row must contain exactly $N_w + N_w'$ non-zero entries, it must have the $s_{n_w}^w$-entries for $1 \leq n_w \leq N_w'$ and the $s_{n_w}^{w*}$-entries for $1 \leq n_w \leq N_w$.

Since $K_w > 2$, we can do further investigation on the third row of $\tilde{\boldsymbol{X}}_{Cw}$. The third row is decided by the first and the second row jointly. Because the first row does not have $s_{N_w'+1}^{w*}, \cdots, s_{N_w}^{w*}$, the third rows can not have any $s_{n_w}^w$-entries, $N_w' + 1 \leq n_w \leq N_w$. Furthermore, because the second row does not have any $s_{n_w}^w$-entries, $N_w' + 1 \leq n_w \leq N_w$, it can be easily shown that the third row can not have any $s_{n_w}^{w*}$-entries, $N_w' + 1 \leq n_w \leq N_w$.

Hence, the third row can only have the $s_{n_w}^w$-entries and the $s_{n_w}^{w*}$-entries for $1 \leq n_w \leq N_w'$. There are at most $2N_w'$ non-zero entries in the third row and it contradicts with the fact that every row in $\tilde{\boldsymbol{X}}_{Cw}$ contains exactly $N_w + N_w'$ non-zero entries. This means that the data-rate of $\tilde{\boldsymbol{X}}_{Cw}$ can not be strictly larger than $1/2$. Because it has been shown that the data-rate of $\tilde{\boldsymbol{X}}_{Cw}$ is lower-bounded by $1/2$, we conclude that the data-rate of $\tilde{\boldsymbol{X}}_{Cw}$ is exactly $1/2$ when $K_w > 2$.

## APPENDIX E

## Proof of Theorem 5

Like in Theorems 3 and 4, we still partition $\boldsymbol{X}_C$ into $\boldsymbol{X}_C = [\boldsymbol{X}_{C1}, \cdots, \boldsymbol{X}_{CW}]$. Let $\boldsymbol{X}_C^k$ denote the matrix containing all the sub-matrices $\boldsymbol{X}_{Cw}$ with $k$ non-zero rows, and hence, $\boldsymbol{X}_C = [\boldsymbol{X}_C^1, \cdots, \boldsymbol{X}_C^K]$. Furthermore, assume the total number of non-zero entries in $\boldsymbol{X}_C^k$ is $P_k$, and hence, $\sum_{k=1}^K P_k$ is the total number of non-zero entries in $\boldsymbol{X}_C$. For convenience, we refer to any entry containing $s_n$ as the $s_n$-entry. Similarly, any entry containing $s_n^*$ is referred to as the $s_n^*$-entry.

In order to derive the upper bound of the data-rate, we first consider the case that $K = 3$. For this case, $\boldsymbol{X}_C^3$ contains at most one sub-matrix and we assume $\boldsymbol{X}_C^3 = \boldsymbol{X}_{C1}$. Thus, $\boldsymbol{X}_C^3$ is a row-monomial DOSTBC-CPI and its data-rate is exactly $1/2$ by Theorem 4. Furthermore, we assume $\boldsymbol{X}_C^3$ is in variables $s_1, \cdots, s_{N_1}$, $1 \leq N_1 \leq N$. By the proof of Theorem 4, every row of $\boldsymbol{X}_C^3$ contains exactly one $s_n$-entry and one $s_n^*$-entry, $1 \leq n \leq N_1$. Therefore, there is no $s_n$-entry or $s_n^*$-entry in $\boldsymbol{X}_C^1$ and $\boldsymbol{X}_C^2$, $1 \leq n \leq N_1$; otherwise, there will be two $s_n$-entries or two $s_n^*$-entries in a row of $\boldsymbol{X}_C$, which will make the noise covariance matrix $\boldsymbol{R}$ non-diagonal. Thus, the matrix $[\boldsymbol{X}_C^1, \boldsymbol{X}_C^2]$ is actually a row-monomial DOSTBC-CPI in variables $s_{n+1}, \cdots, s_N$. Furthermore, because every column in the matrix $[\boldsymbol{X}_C^1, \boldsymbol{X}_C^2]$ has at most two non-zero entries, it is easy to show that its data-rate can not be larger than $1/2$ by following the proof of Theorem 2 in [1]. Because the data-rate of $\boldsymbol{X}_C^3$ is exactly $1/2$ and the data-rate of $[\boldsymbol{X}_C^1, \boldsymbol{X}_C^2]$ is less than $1/2$, the data-rate of $\boldsymbol{X}_C = [\boldsymbol{X}_C^1, \boldsymbol{X}_C^2, \boldsymbol{X}_C^3]$ must be upper-bounded by $1/2$ when $K = 3$.

Secondly, we consider the case that $K > 3$. When $k > 2$, the data-rate of $\boldsymbol{X}_C^k$ is exactly $1/2$. This means, if an information-bearing symbol $s_n$ appears in a row of $\boldsymbol{X}_C^k$, it appears exactly twice. On the other hand, (29) implies that every row of $\boldsymbol{X}_C$ must have the information-bearing symbol $s_n$ for at least once, $1 \leq n \leq N$. Therefore, the following inequality holds

$$\sum_{k=1}^2 P_k + \sum_{k=3}^K \frac{P_k}{2} \geq NK. \tag{E.1}$$

On the other hand, there are totally $P_k/k$ columns in $\boldsymbol{X}_C^k$. Thus, the total number $T$ of columns in $\boldsymbol{X}_C = [\boldsymbol{X}_C^1, \cdots, \boldsymbol{X}_C^K]$ is given by

$$T = \sum_{k=1}^K \frac{P_k}{k}. \tag{E.2}$$

By (E.1) and (E.2), it is easy to obtain $2N \leq T$ under the assumption that $K > 3$, and hence, the data-rate of $\boldsymbol{X}_C$ is upper-bounded by $1/2$ when $K > 3$.

REFERENCES

[1] Z. Yi and I.-M. Kim, "Single-symbol ML decodable distributed STBCs for cooperative networks," *IEEE Trans. Inform. Theory*, vol. 53, pp. 2977–2985, Aug. 2007.

[2] A. Sendonaris, E. Erkip, and B. Aazhang, "User cooperation diversity–Part I: System description," *IEEE Trans. Commun.*, vol. 51, pp. 1927–1938, Nov. 2003.

[3] ——, "User cooperation diversity–Part II: Implementation aspects and performance analysis," *IEEE Trans. Commun.*, vol. 51, pp. 1939–1948, Nov. 2003.

[4] J. N. Laneman, D. N. C. Tse, and G. W. Wornell, "Cooperative diversity in wireless networks: Efficient protocols and outage behavior," *IEEE Trans. Inform. Theory*, vol. 50, pp. 3062–3080, Dec. 2004.

[5] J. N. Laneman and G. W. Wornell, "Energy-efficient antenna sharing and relaying for wireless networks," in *Proc. of WCNC 2000*, vol. 1, Sep. 2000, pp. 7–12.

[6] Md. Z. A. Khan and B. S. Rajan, "Single-symbol maximum likelihood decodable linear STBCs," *IEEE Trans. Inform. Theory,* vol. 52, pp. 2062–2091, May 2006.

[7] P. A. Anghel and M. Kaveh, "Exact symbol error probability of a cooperative network in a rayleigh-fading environment," *IEEE Trans. Wireless Commun.*, vol. 3, pp. 1416–1421, Sep. 2004.

[8] A. Ribeiro, X. Cai, and G. B. Giannakis, "Symbol error probabilities for general cooperative links," *IEEE Trans. Wireless Commun.*, vol. 4, pp. 1264–1273, May 2005.

[9] M. O. Hasna and M. S. Alouini, "End-to-end performance of transmission systems with relays over rayleigh–fading channels," *IEEE Trans. Wireless Commun.*, vol. 2, pp. 1126–1131, Nov. 2003.

[10] ——, "Harmonic mean and end-to-end performance of transmission systems with relays," *IEEE Trans. Commun.*, vol. 52, pp. 130–135, Jan. 2004.

[11] D. Chen and J. N. Laneman, "Modulation and demodulation for cooperative diversity in wireless systems," *IEEE Trans. Wireless Commun.*, vol. 5, pp. 1785–1794, July 2006.

[12] I. Hammerström, M. Kuhn and A. Wittneben, "Impact of relay gain allocation on the performance of cooperative diversity networks," in *Proc. IEEE VTC'04*, vol. 3, Sept. 2004, pp. 1815–1819.

[13] Z. Yi and I.-M. Kim, "Joint optimization of relay-precoders and decoders with partial channel side information in cooperative networks," *IEEE J. Sel. Areas Commun.*, vol. 25, pp. 447–458, Feb. 2007.

[14] Y. Zhao, R. Adve, and T. J. Lim, "Symbol error rate of selection amplify-and-forward relay systems," *IEEE Commun. Lett.*, vol. 10, pp. 757–759, Nov. 2006.

[15] ——, "Improving amplify-and-forward relay networks: Optimal power allocation versus selection," *IEEE Trans. Wireless Commun.*, accepted for publication.

[16] Z. Yi and I.-M. Kim, "Diversity order analysis of the decode-and-forward cooperative networks with relay selection," *IEEE Trans. Wireless Commun.*, submitted for publication.

[17] J. N. Laneman and G. W. Wornell, "Distributed space-time-coded protocols for exploiting cooperative diversity in wireless networks," *IEEE Trans. Inform. Theory*, vol. 49, pp. 2415–2425, Oct. 2003.

[18] R. U. Nabar, H. Bölcskei, and F. W. Kneubühler, "Fading relay channels: Performance limits and space-time signal designs," *IEEE J. Sel. Areas Commun.*, vol. 22, pp. 1099–1109, Aug. 2004.

[19] S. Yang and J.-C. Belfiore, "Optimal space-time codes for the MIMO amplify-and-forward cooperative channel," *IEEE Trans. Inform. Theory*, vol. 53, pp. 647–663, Feb. 2007.

[20] H. El Gamal and D. Aktas, "Distributed space-time filtering for cooperative wireless networks," in *Proc. IEEE GLOBECOM'03*, vol. 4, Dec. 2003, pp. 1826–1830.

[21] S. Yiu, R. Schober, and L. Lampe, "Distributed space-time block coding," *IEEE Trans. Commun.*, vol. 54, pp. 1195–1206, July 2006.

[22] A. Murugan, K. Azarian and H. El Gamal, "Cooperative lattice coding and decoding," *IEEE J. Sel. Areas Commun.*, vol. 25, pp. 268–279, Feb. 2007.

[23] Y. Jing and B. Hassibi, "Distributed space-time coding in wireless relay networks," *IEEE Trans. Wireless Commun.*, vol. 5, pp. 3524–3536, Dec. 2006.

[24] Y. Li and X.-G. Xia, "A family of distributed space-time trellis codes with asynchronous cooperative diversity," *IEEE Trans. Commun.*, vol. 55, pp. 790–800, April 2007.

[25] M. O. Damen and A. R. Hammons Jr., "On distributed space-time coding," in *Proc. IEEE WCNC'07*, Mar. 2007, pp. 552–557.

[26] T. Kiran and B. S. Rajan, "Partially-coherent distributed space-time codes with differential encoder and decoder," *IEEE J. Sel. Areas Commun.*, vol. 25, pp. 426–433, Feb. 2007.

[27] Y. Hua, Y. Mei, and Y. Chang, "Wireless antennas-making wireless communications perform like wireline communications," in *Proc. IEEE AP-S Topical Conference on Wireless Communication Technology*, Oct. 2003, pp. 47–73.

[28] G. S. Rajan and B. S. Rajan, "Distributed space-time codes for cooperative networks with partial CSI," in *Proc. IEEE WCNC'07*, Mar. 2007, pp. 902–906.

[29] Y. Jing and H. Jafarkhani, "Using orthogonal and quasi-orthogonal designs in wireless relay networks," *IEEE Trans. Inform. Theory*, accepted for publication, July, 2007.

[30] W. Su and X.-G. Xia, "On space-time block codes from complex orthogonal designs," *Wireless Personal Commun.*, vol. 25, pp. 1–26, Apr. 2003.

[31] V. Tarokh, H. Jafarkhani, and A. R. Calderbank, "Space-time block codes from orthogonal designs," *IEEE Trans. Inform. Theory,* vol. 45, pp. 1456–1467, July 1999.

[32] H. Wang and X.-G. Xia, "Upper bounds of rates of complex orthogonal space-time block codes," *IEEE Trans. Inform. Theory,* vol. 49. pp. 2788–2796, Oct. 2003.

[33] P. Elia and P. V. Kumar, "Approximately universal optimality over several dynamic and non-dynamic cooperative diversity schemes for wireless networks," *IEEE Trans. Inform. Theory,* submitted for publication, Dec. 2005.

[34] S. Alamouti, "A simple transmit diversity technique for wireless communications," *IEEE J. Sel. Areas Commun.*, vol. 16, pp. 1451–1458, Aug. 1998.
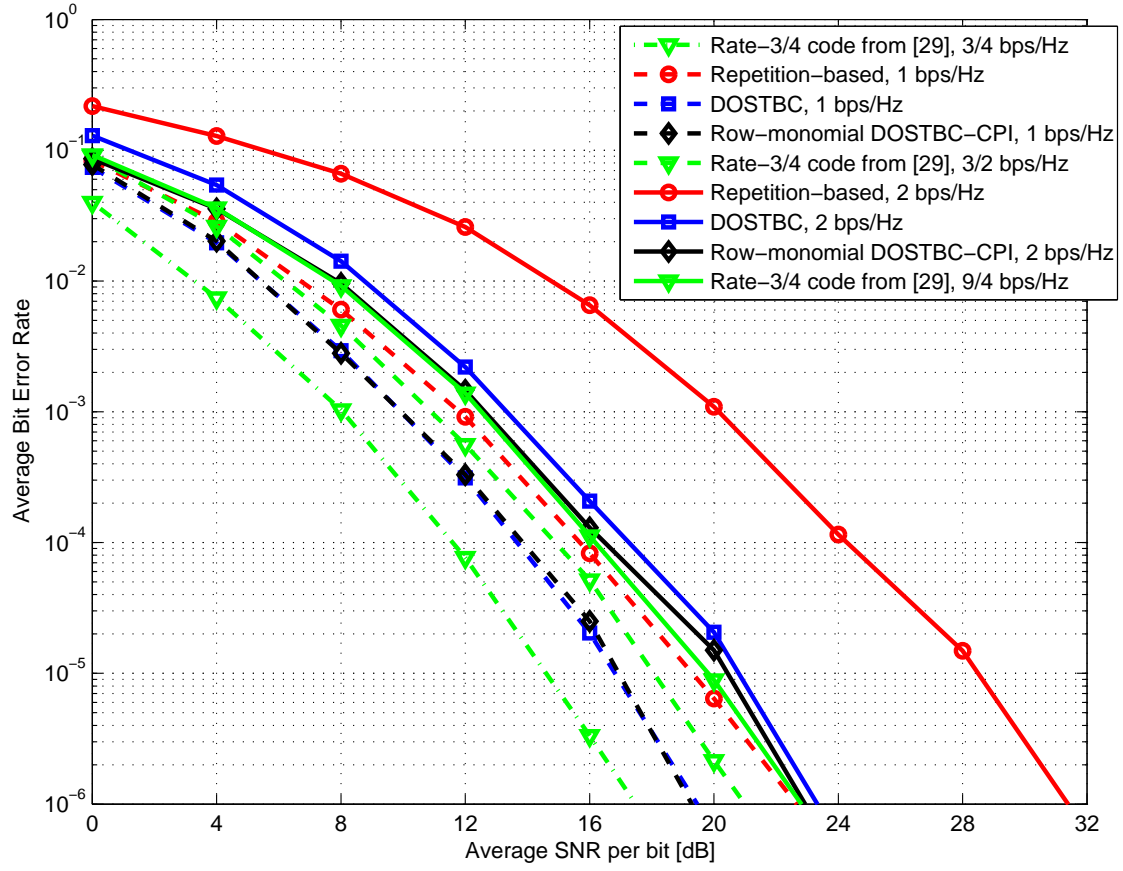
Fig. 1. Comparison of the rate-$3/4$ code from [29], the DOSTBCs, the row-monomial DOSTBCs-CPI, and the repetition-based cooperative strategy, $N = 4$, $K = 4$.
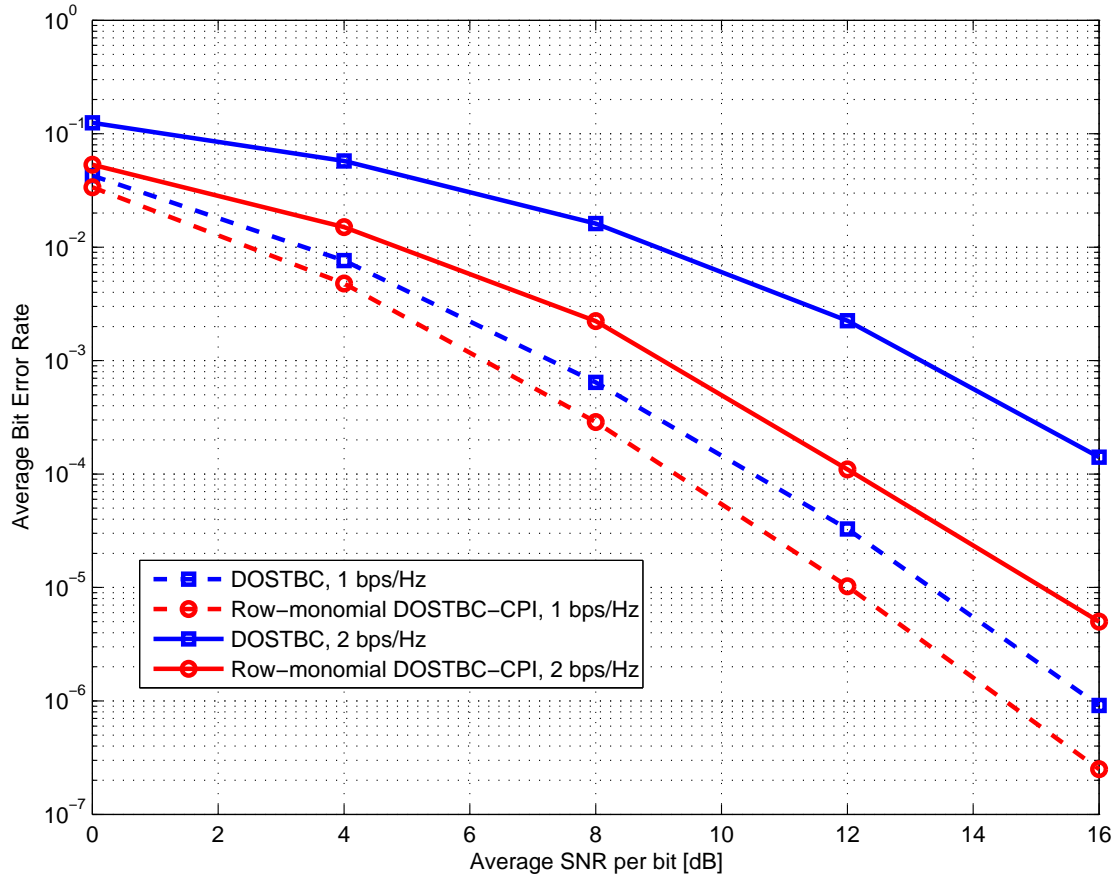
Fig. 2. Comparison of the DOSTBCs and the row-monomial DOSTBCs-CPI, $N = 8$, $K = 6$.